Pol. J. Environ. Stud. Vol. 27, No. 4 (2018), 1573-1581
DOI: *10.15244/pjoes/77079* ONLINE PUBLICATION DATE: 2018-02-23

Original Research

Analysis of Environmental Factors Affecting Variation in Interrill Erosion under Rainfall Simulation

Ali Bagherian Kalat[1], Gholam Reza Lashkaripour[2]*, Mohammad Ghafoori[2], Ali Akbar Abbasi[3]

[1]Engineering Geology of Ferdowsi University of Mashhad International Campus, Mashhad, Iran
[2]Department of Geology, Faculty of Science, Ferdowsi University of Mashhad, Mashhad, Iran
[3]Department of Civil Engineering, Islamic Azad University, Branch of Boojnord, Boojnord, Iran

Received: 19 July 2017
Accepted: 18 September 2017

Abstract

This research was carried out to determine the influence of rainfall intensity and soil physico-chemical properties on erosion behavior of 11 representative soil samples from the badlands of the Dahanghale area in northeastern Iran. Soil textures were loamy to silty loamy, with a very heterogeneous surface gravel and vegetation cover. The research was studied under two simulated rainfall intensities: 37 and 48 mm h^{-1} for 10- and 25-year return periods, respectively, during 30 minutes. The results revealed that gypsiferous red beds (Ngr) parent material develops the most erodible surfaces while conglomerate (Pgc) contributes the least sediment yield. Values of mean measured soil loss varied from 30.3 to 559.1 g m^{-2} for rain storms of 37 mm h^{-1}, and under rain storms of 48 mm h^{-1} the values of mean soil loss varied from 62.4 to 1,135.9 g m^{-2}. The soil loss significantly increased as rainfall intensity increased. Finally, the results of research showed that the nature of parent rocks and rainfall intensity can greatly affect soil erosion processes. Based on the finding of research we can conclude that some physico-chemical properties of study soils and soil vegetation and rock fragment cover are suitable indicators for predicting soil loss in the Dahanghale watershed.

Keywords: rainfall intensity, semiarid ecosystem, soil loss

Introduction

Rain erosivity and soil erodibility are factors that control intensity of soil erosion. Intense rainfall and runoff events cause most soil erosion and sediment yield [1], and consequently gully and badland development. In interrill erosion, the main processes are detachment of soil material by raindrop impact and transport of sediment by sheet flow [2]. The intensity of interrill erosion is related to many factors, namely, rainfall intensity and kinetic energy, infiltration and runoff rates, soil characteristics, and soil surface conditions [3-6].

Due to the high susceptibility to erosion, badland areas have high erosion rates despite occupying relatively small areas, and can make disproportionate contributions to watershed scale sediment budgets [7]. Critical source

*e-mail: Lashkaripour@um.ac.ir

areas are usually associated with marls, clay rocks, mudstone, and shale [8]. Additionally, a few reports have shown that badland landforms are on sands or poorly consolidated sandstone [9-10]. In highly eroded soils, sediment yield and nutrient release have a significant role on the degradation of water quality and eutrophication in large shallow lakes [11].

In critical source areas, considerable spatial and temporal variability in runoff generation and erosion processes have been reported [8, 12]. Spatial patterns in rates of soil loss and sediment yield in badlands result from lithological controls [13], soil vegetation cover [14], antecedent soil moisture [15], soil physico-chemical characteristics (high dispersivity) – including mineralogy [2, 12, 16-19], and soil surface roughness [13]. Additionally, climatic conditions – especially rainfall intensity – have a direct effect on soil erosion processes, sediment yield rates, and, consequently, gully and badland development [5, 20-22].

Rainfall simulation is a good method for comparing and quantifying different runoff and erosion processes and factors that influence them. Numerous researchers have used simulated rainfall experiments on a wide range on badland areas [3, 20, 23].

The erodible lithologies include about 60 percent of the area of the Dahanghale watershed basin. Securitizing available literature about effective factors on soil erosion in eroded soils shows that in spite of numerous reports on different soil erosion processes, little comparative study has been considered on sediment yield originating from soils with different parent material in plot scale under different rainfall intensities. So, there is a need for more detailed investigation on soil physico-chemical and vegetation properties that effect soil erosion. Accordingly, the present study was carried out to comprehensively compare the effects of environmental factors and rainfall intensities controlling spatial variation in soil loss in Dahanghale drainage watershed. Due to the serious erosion of soft salt-rich sedimentary rock outcrops, high sediment discharge reduced the water capacity of Dahanghale Reservoir dam. Rainfall simulation experiments were carried out with two intensities: 37 and 48 mm h^{-1} during 30 minutes. The main objectives of this research (at the plot scale) are as follows:

A) Study relationship between soil loss and rainfall intensity.
B) Determine relationship between soil loss and soil physical and chemical characteristics.
C) Study relationship between soil loss and soil vegetation and rock fragment cover.

Material and Methods

Study Area

This study was carried out in the Dahanghale Watershed (1850 Km^2) of Khorasane Razavi Province in northeastern Iran (Fig. 1). This watershed is characterized by moderately steep slopes of semiarid climate. Annual precipitation is about 220 mm. The predominant lithologies are marl, flysch type rocks, conglomerate, and intermediate volcanic rocks. In the arid to semiarid

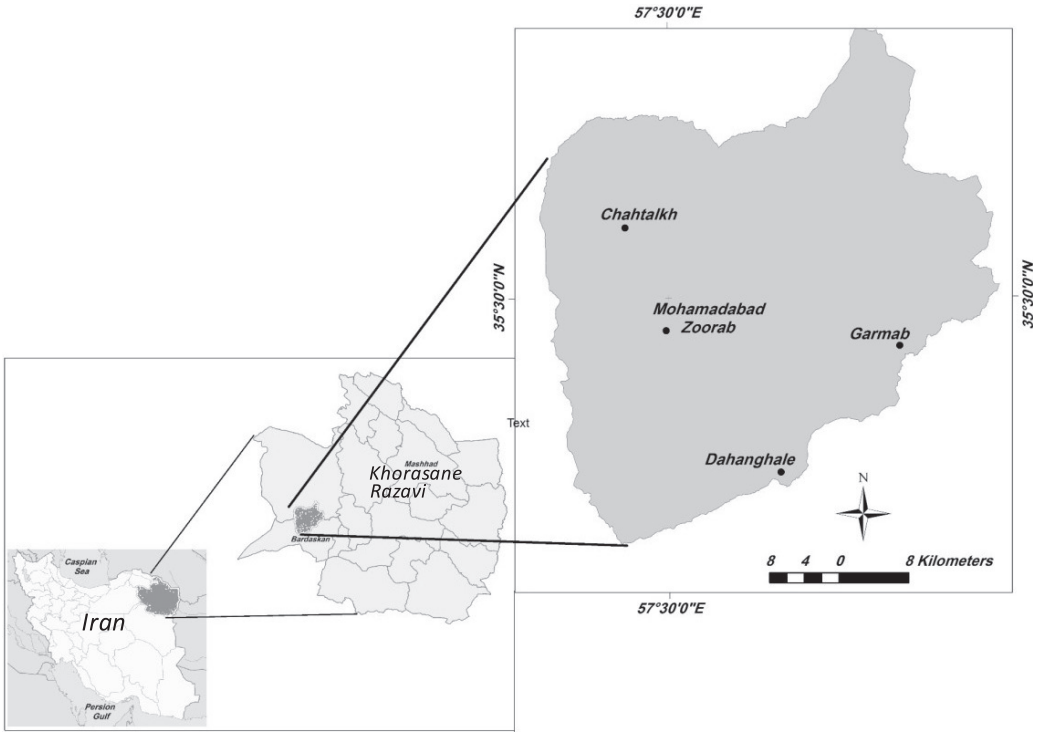

Fig. 1. Location of study area in Khorasane Razavi province, Iran.

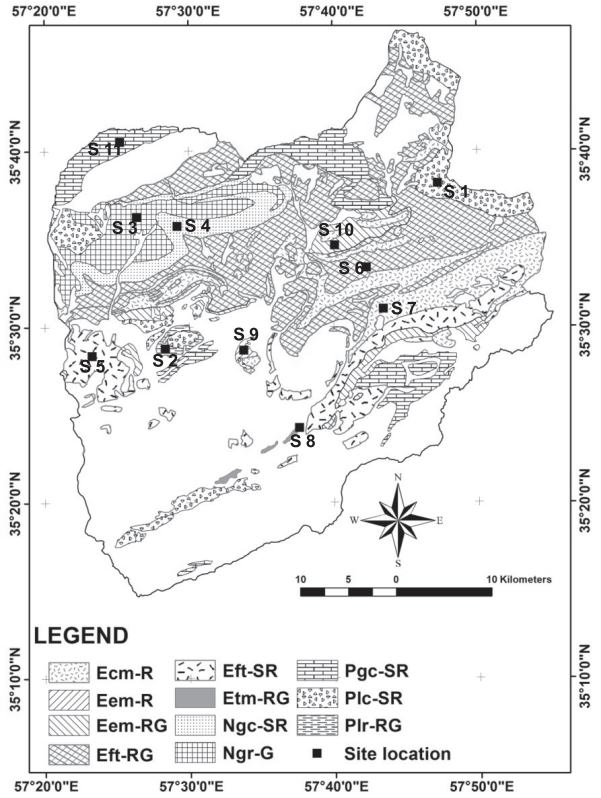

Fig. 2. Location of 11 experimental sites on a working map.

ecosystem of the area the flora of watershed dominantly includes Cousinia, Artemisia Siberi, Acantholimon, Astragalus microcephulus, Salsola Sp., and Amygdalus lycoides [24]. The soil profiles are poorly developed. The soils have Regosol units according to FAO soil classification with loamy to silty loam textures.

Plot Locations and Characteristics

For specifying location of the plots, geology, slop, land use, and erosional facies maps were prepared using 1:50,000 topography maps [25], Landsat 8.0 ETM^+ satellite imagery (taken on 23 February 2013 with spatial resolution of 30 m) and field surveying. 11 different locations were selected for these experiments on the basis of differences in geology and erosion facies (Fig. 2). The plots located on erodible parent materials consisted of marl, conglomerate, and Tuff. These 11 test sites had the same slope (slope gradients of 14°) and land use (rangeland), but different lithology and erosion facies. The characteristics of 11 experimental sites, including lithology, erosion facies, and vegetation cover, are shown in Table 1. In all working polygons, rainfall simulations were carried out in autumn 2016.

Experiment Design

The rainfall simulator that was used in this study is a portable non-pressurized rainfall simulator developed at the Soil Conservation and Watershed Management Research Institute (SCWMRI) in Iran as detailed by [26]. The basic unit of the simulator is a plexiglass container with two plates (1.2 m long x 0.84 m wide) at the top and bottom connected with a frame of 0.04 m height (Fig. 3).

Table 1. Lithology, predominant erosion, and vegetation cover characteristics of the 11 experimental sites in Dahanghale Watershed.

No.	Lithology (Parent rocks)	Predominant erosion facies	Vegetation types	Mean vegetation cover (%)	Mean rock fragment cover (%)	(Experimental sites)
1	Neogene conglomerate (Plc)	Sheet-Rill (SR)	*Cousinia Acantholimon*	12.6	25.7	Plc-SR
2	Red marl (Plr)	Rill-Gully (RG)	*Salsola Sp.*	0.7	2.3	Plr-RG
3	Gypsiferous red beds (Ngr)	Gully (G)	*Salsola Sp. Ephedra Sp.*	0	5.7	Ngr-G
4	Conglomerate (Ngc)	Sheet-Rill (SR)	*Astragalus Sp. Cousinia*	10.3	21.3	Ngc-SR
5	Flysch type rocks (Eft)	Sheet-Rill (SR)	Astragalus Sp. Acantholimon	9	17.7	Eft- SR
6	Flysch type rocks (Eft)	Rill-Gully (RG)	*Astragalus Sp. Acantholimon*	6.3	12.3	Eft-RG
7	Conglomerate, marl (Ecm)	Sheet-Rill (SR)	*Amygdalus Sp. Cousinia*	8.6	19.0	Ecm- SR
8	Green tuff and marl (Etm)	Rill-Gully (RG)	*Salsola Sp.*	3.6	6.3	Etm-RG
9	Evaporite with green marl (Eem)	Rill (R)	*Salsola Sp. Ephedra Sp.*	2.3	5.0	Eem-R
10	Evaporite with green marl (Eem)	Rill-Gully (RG)	*Salsola Sp. Ephedra Sp.*	1.6	2.0	Eem-RG
11	Paleogene conglomerate (Pgc)	Sheet-Rill (SR)	*Astragalus Sp. Cousinia*	13.6	32.3	Pgc-SR

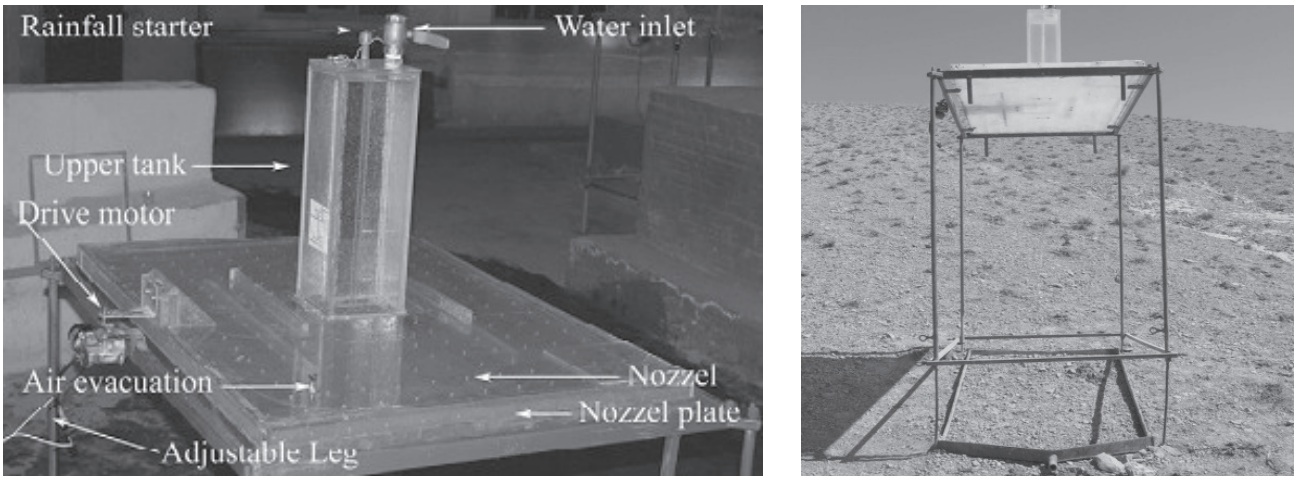

Fig. 3. Photograph of rainfall simulator and its different parts (left) and the used rainfall simulator in the field (right).

The lower raindrop-former plate contains 216 nozzles of 0.5 mm diameter, which are spaced 0.07 m apart. The oscillating mechanism of the simulator works with a drive motor to produce a uniform distribution of raindrops across the plot. With an upper tank of 11.28 L, the whole capacity of the simulator is 51.6 L. Four adjustable legs, 1.5 m in height, help to mount the system horizontally on various land slopes. Drops form by gravity and atmospheric pressure controlled by a tube connecting the basic unit to the outside within the upper tank. This gives a 3.6 mm median drop size and a nozzle exit velocity of 10 to 80 ms^{-1}. Fig. 3 shows the mounted rainfall simulator in the field.

Two rainfall intensities of 37.3 and 48.2 mm h^{-1} and 30 min duration are the most frequent rainfalls in the study area. So, 37 and 48 mm h^{-1} were chosen as the intensities for 10- and 25-year return periods, respectively, to be produced by the rainfall simulator. All rainfall intensities were used by the rainfall simulator in three replications.

The rainfall simulation experiments were performed during autumn 2016, when soil moisture values were between 4.04% and 11.72%. 66 rainfall simulations with two intensities (37 and 48 mm h^{-1}) were simulated for a period of 30 minutes at 11 locations in the study area. In each experimental site the locations of the experiments at different rainfall intensities were selected adjacent to each other. So, they were similar in terms of soil properties, and especially in antecedent soil water content. All 66 runoff and sediment data points were collected and analyzed in the laboratory.

Before performing the simulations, in order to determine effective factors in sediment production and erosion 33 soil representative samples from the first 10 cm depth of soil were taken and analyzed [23]. Soil texture was determined by the sieve and pipette method; pH (H_2O) and electrical conductivity (EC) of soil measured by potentiometer in a 1:2.5 and 1:5 soil: deionized water solutions, respectively [27]. Soluble salts investigated on 1:5 crushed soil-water extracts by means of atomic

Table 2. Mean physico-chemical characteristics of soils in the 11 experimental sites.

No.	Working polygons (experimental sites)	Sand (%)	Silt (%)	Clay (%)	Soil texture	pH	EC (dSm^{-1})	SAR	Soil vertical resistance ($Kg\ cm^{-2}$)
1	Plc-SR	42	42	16	Loam	7.97	1.50	4.3	2.89
2	Plr-RG	30	51	19	Silty Loam	8.10	12.53	31.1	1.04
3	Ngr-G	27	54	19	Silty Loam	8.43	85.70	166.6	0.46
4	Ngc-SR	43	40	17	Loam	7.80	0.96	3.6	2.45
5	Eft- SR	41	40	19	Loam	7.77	1.21	2.8	3.24
6	Eft-RG	33	45	22	Loam	8.00	3.31	4.5	1.81
7	Ecm- SR	45	37	18	Loam	7.83	0.94	1.9	2.98
8	Etm-RG	33	44	23	Loam	8.07	4.12	9.0	1.58
9	Eem-R	27	51	22	Silty Loam	8.13	8.51	18.8	1.46
10	Eem-RG	26	56	18	Silty Loam	8.30	50.30	99.2	1.19
11	Pgc-SR	43	39	18	Loam	7.83	0.82	3.1	3.61

Table 3. Analysis of variance (ANOVA) for the soil loss amounts in different soils in 37 and 48 mm h^{-1} rainfall intensities

Rainfall intensity (mm h^{-1})		Sum of squares	df	Mean square	F	Sig.
37	Between groups	721,893.913	10	72,189.391	65.215	0.000
	Within groups	24,352.790	22	1,106.945		
	Total	746,246.702	32			
48	Between groups	728,585.722	10	72,858.572	22.304	0.000
	Within groups	71,865.584	22	3,266.617		.
	Total	800,451.305	32			

df = degrees of freedom

absorption spectrophotometry for Ca^{+2}, Mg^{+2}, Na^{+}, and K^{+}, and ion chromatography for Cl^{-}, SO_4^{-2}, and HCO_3^{-} [28]. Sodium adsorption ratio (SAR) was calculated according to Equation 1 (all cations as $meql^{-1}$):

$$S.A.R. = \frac{Na^{+}}{\sqrt{1/2(Ca^{2+} + Mg^{2+})}} \quad (1)$$

The vertical resistance of soil surface (VRS) was measured by using a pocket penetrologger from Eijkelkamp (the Netherlands) [29]. In experimental plots some soil surface conditions such as vegetation cover and rock fragment (%) were visually estimated. Antecedent soil moisture in all plots was measured from the first 10 cm depth by oven drying before the start of experiments.

Statistical Analysis

The statistical analysis of data was conducted with SPSS 22 software for Windows. Normalization distribution was tested. One-way analysis of variance (ANOVA) techniques were used by Duncan multiple range test with a level of significance of $p \leq 0.05$.

For determining the degree and type of correlation between sediment yield and soil physico-chemical properties and soil surface cover we used Pearson's correlation matrix (r) and multi-variable regression method [26]. The independent-samples t-Test was used to evaluate the difference between the means of soil loss under two simulated rainfall intensities. Stepwise multiple regression analysis was used to assess the effect of soil physico-chemical properties and soil surface cover on soil loss. In applying stepwise multiple regression analysis, soil loss was considered the dependent variable and each soil physico-chemical property and soil surface cover was an independent variable.

Results and Discussion

Table 2 shows some physico-chemical plot specifications such as soil texture, pH, EC, SAR, and SVR of soils in the 11 experimental sites overlaying different parent rocks.

A wide range in mean soil loss (g m^{-2}) was observed for 11 soil experimental plots (Fig. 4). The values of mean measured soil loss vary from 30.26 to 559.19 g m^{-2} for a 37 mm h^{-1} rain storm. Under a 48 mm h^{-1} rain storm the

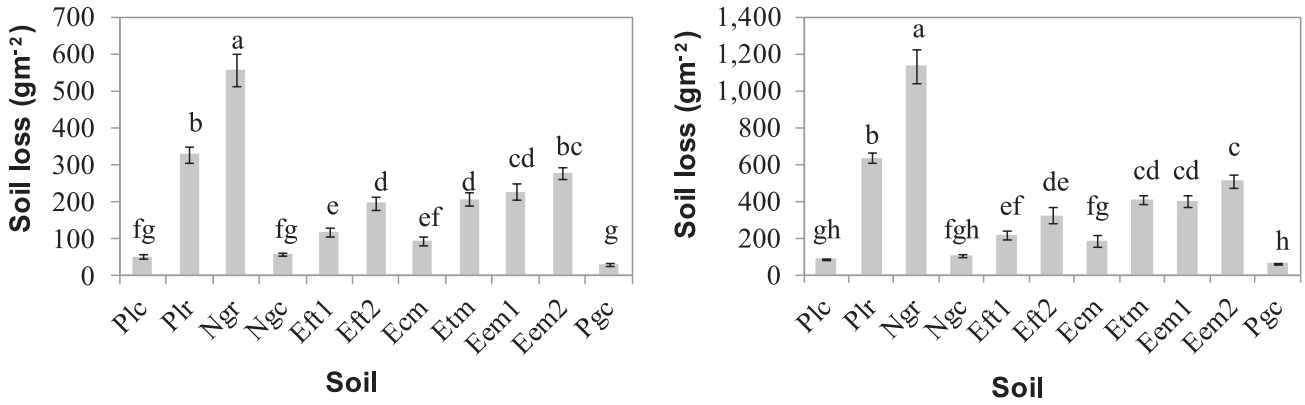

Fig. 4. The mean soil loss (g m^{-2}) obtained from different soils in 11 experimental sites under 37 (left) and 48 mm h-1 (right) rainfall intensity experiments; values followed by lowercase letters are significantly different for $\alpha<0.05$ using the Duncan method (bars represent standard error of means value of soil loss).

Table 4. t-Test results from experimental sites for soil loss.

Rainfall Intensity (mm h^{-1})	n	Mean (g m^{-2})	SD	SE	P	t	Diff.[a]	df
37	33	195.66	152.70	26.58	<0.005	-2.94	-175.99	47
48	33	371.66	307.38	53.68				

Diff.[a] = difference in g m^{-2} between the means

values of mean soil loss vary from 62.40 to 1,135.95 g m^{-2} (Fig. 4). The gypsiferous red beds (Ngr) parent material develops the most erodible surfaces while conglomerate (Pgc) contributes the least soil loss. In fact, under rainfall intensity of 37 mm h^{-1} soil loss for Ngr, with an average value of 1,135.95 g m^{-2}, was more than 18 times higher than that of Pgc. At 48 mm h^{-1}, sediment yield for the Ngr, with an average value of 559.2 g m^{-2}, was more than 17 times higher than that of Pgc.

Analysis of variance (ANOVA) shows there are significant differences between treatments (different soils overlaying parent rocks) in soil loss ($P<0.05$) (Table 3). Therefore, it was found that the soil factors significantly affected soil loss. The Duncan multiple-range test analysis shows mean soil loss in different soils are significantly different for a level of significance of $p<0.05$ (Fig. 4).

The effect of the impact and splashing of rain drops is an important factor causing soil detachment and sediment yield [2]. Many researchers have reported that rainfall intensity is an important factor affecting soil erosion (3-5, 16). Our study shows that the relationship between rainfall intensity and mean soil loss is positive and significant (Table 4). It can be clearly observed from the independent-samples t-Test analysis that the effect of rainfall intensity on soil loss is significant (Table 4).

For the coefficient of correlation matrix of soil loss, increase the coefficient of correlation of the 11 soil locations in the study under two rainfall simulation intensities (Table 5). The variables of vegetation and rock fragment cover are the efficient variables that have a strong negative correlation with soil loss. Rock fragment cover contributed to delayed runoff flow and increased infiltration rates, diminishing soil loss rates. Similarly, vegetation cover protects the surface from raindrop impact, controls the surface infiltration rate, and reduces surface runoff, sediment detachment, and transport. The results are in agreement with the studies of El Kateb et al. [30] and Zavala et al. [32].

The finding of this research on the role of the silt and sand portion of soil on soil erosion is similar to Vahhabi and Nikkami [26] (Table 5), i.e., soil erodibility increases as sand content decreases ($r = -0.772$) and silt content increases ($r = 0.752$). Soils differ in their susceptibility to erosion (erodibility) based on texture, and soils with a high percentage of silt particles have greater erodibility than sandy or clay soil under the same conditions. Sandy soil generally has high infiltration capacity and low transportability, which results in reduced runoff production, particle transport, and, consequently, erosion (intensity). Medium-textured soils are more erodible. As these soils tend to produce increased runoff, soil particles are easily detached and transported [33].

The influence of antecedent soil water content on soil erosion is still a matter of debate, as opposing effects have been reported on aggregate breakdown and seal formation [34]. However, a significant effect of antecedent soil moisture on runoff generation has been reported. Wet soils double the runoff coefficient and shorten the time to runoff, compared with the same soils when dry [35].

Table 5. Coefficients of correlation matrix of soil loss and soil properties.

Rainfall intensity (mm h^{-1})	Parameter	Vegetation cover (%)	Rock fragment cover (%)	Moisture (%)	Soil vertical resistance (Kg cm^{-2})	Clay (%)	Silt (%)	Sand (%)	EC (dSm^{-1})	pH	SAR
37	Pearson correlation	-0.839**	-0.736**	0.785**	-0.868**	0.222	0.752**	-0.772**	0.849**	0.816**	0.856**
	Sig. (2-tailed)	0.000	0.000	0.000	0.000	0.215	0.000	0.000	0.000	0.001	0.000
	N	33	33	33	33	33	33	33	33	33	33
48	Pearson correlation	-0.818**	-0.826**	0.769**	-0.858**	0.189	0.723**	-0.734**	0.850**	0.847**	0.856**
	Sig. (2-tailed)	0.000	0.000	0.000	0.000	0.293	0.000	0.000	0.000	0.000	0.000
	N	33	33	33	33	33	33	33	33	33	33

**denotes that probability (Pr) ≤ the level of significance at 0.01

Table 6. Coefficient of soil loss for 37 and 48 mm h^{-1} rainfall intensities.

Rainfall intensity (mm h^{-1})	Parameter	Unstandardized coefficients		Standardized coefficients	t	Sig.
		B	Std. error	Beta		
37	Constant	292.405	29.486		9.917	.000
	Vertical resistance of soil surface	-38.033	16.798	-.258	-2.264	.031
	Sodium adsorption ratio	1.408	.216	.483	6.517	.000
	Vegetation cover	-9.895	3.116	-.331	-3.176	.004
48	Constant	559.974	69.940		8.006	.000
	Vertical resistance of soil surface	-84.774	41.040	-.261	-2.066	.048
	Sodium adsorption ratio	2.952	.480	.501	6.145	.000
	Vegetation cover	-18.183	6.946	-.299	-2.618	.014

In our research the factor of antecedent soil moisture shows a positive correlation (r = 0.785) with soil loss (Table 5). The hydraulic gradient decreases as soil moisture content increases. The reduction in the infiltration rate causes higher runoff and consequently higher soil loss. Similar findings have been reported by Ziadat et al. [36].

As Table 5 shows, soil loss shows a positive correlation with Ec (r = 0.849), SAR (r = 0.856), and pH (r = 0.816). The same results were noted by De Santis et al. [37] and Pulice et al. [38], who reported that some physico-chemical properties of the soil such as pH, EC, and SAR well explain the dominance of concentrated water erosion.

In this research, regression analysis was used to examine the relative contribution of soil physico-chemical properties on soil loss (Table 6). The results present the variables of vertical resistance of soil surface (VRS), sodium adsorption ratio (SAR), and vegetation cover (VC) having a greater contribution in explaining the variations in soil loss.

Equations (2) and (3), with determination coefficients of 0.92 (R^2_1) and 0.90 (R^2_2) ($p<0.01$), were selected as appropriate models for predicting soil loss for the 37 and 48 mm h^{-1} rainfall intensity, respectively.

$$SY = -38.03\ (VRS) + 1.41\ (SAR) - 9.89\ (VC) + 292.41 \quad (2)$$

$$SY = -84.77\ (VRS) + 2.95\ (SAR) - 18.18\ (VC) + 559.97 \quad (3)$$

In equations (2) and (3), SY is the amount of soil loss (g m^{-2}), VRS is the vertical resistance of soil surface (kg cm^{-2}), SAR is the sodium adsorption ratio, and VC is vegetation cover (%).

In these models, $R^2_1 = 0.92$ and $R^2_2 = 0.90$ indicate 92% and 90% of the observed dissipation in dependent variables, respectively. Meanwhile, these models can be justified by the three independent variables that indicate the model's high predictive capability.

Conclusion

In this research we analyzed the spatial variability in soil loss for 11 representative selected soil samples derived from different parent rocks. The results revealed that rainfall simulation is well adapted to the analysis of rainfall-erosion processes within the study area. Using a portable rainfall simulator revealed the effects on soil loss under two varied rainfall intensities. Soils derived from gypsiferous marl parent rocks and conglomerate rocks showed the most and the least soil loss, respectively. ANOVAs showed that there are significant differences between treatments (different soils) in soil loss ($P<0.01$).

Multiple regression analysis revealed that for applied rainfall intensities of 37 and 48 mm h^{-1}, vertical resistance of soil surface (VRS), sodium adsorption ratio (SAR), and vegetation cover (VC) are the most efficient factors determining soil loss.

Pearson's correlation analysis showed that vegetation and rock fragment cover, soil vertical resistance, and sand fraction are the efficient variables that have negative correlation with soil loss, and the variables of silt fraction and antecedent soil moisture are the variables that have a positive correlation with soil loss. Meanwhile, the factors of SAR, EC, and pH are efficient chemical variables that have a positive correlation with soil loss.

In this study, results of the experiments show that the magnitude of soil loss was highly not only controlled by rainfall intensity but also some soil physical and chemical properties and soil vegetal and rock fragment cover influences the soil loss. So, the mechanism of erosion involves the nature of the parent rocks, soil physico-chemical characteristics, and ground cover.

Consequently, the finding of this research indicates that some physico-chemical properties of study soils and soil vegetation and rock fragment cover are suitable indicators for predicting soil loss in the study area.

Acknowledgements

This study was supported by the Khorasan Razavi Agricultural and Natural Resources Research and Education Center of Iran. We are grateful to all the staff of this Research and Education Center for their help in the investigation, and to Dr. Hamzeh Noor for help in writing the manuscript.

References

1. BARREIRO-LOSTRES F., MORENO A., GONZALEZ-SAMPERIZ P., GIRALT S., NADAL-ROMERO E., VALERO-GARCES B. Erosion in Mediterranean mountain landscapes during the last millennium: a quantitative approach based on lake sediment sequences (Iberian Range, Spain). Catena, **149** (3), 782, **2017**.
2. VAEZI A.R., AHMADI M., CERDA A. Contribution of raindrop impact to the change of soil physical properties andwater erosion under semiarid rainfalls. Science of the Total Environment. **2017**. DOI: 10.1016/j.scitotenv.2017.01.078.
3. MARTINEZ-MURILLO J.F., NADAL-ROMERO E., REGUES D., CERDA A., POESEN J. Soil erosion and hydrology of the western Mediterranean badlands throughout rainfall simulation experiments: a review. Catena, **106**, 101, **2013**.
4. NADAL-ROMERO E., LASANTA T., DE LUIS M., GARCIA-RUIZ J.M. The effect of intense rainstorm events on the suspended sediment response under various land uses: the Aisa valley experimental station. Cuad. Investig. Geography, **38**, 27, **2012**.
5. SHEN H., ZHENG F., WEN L., HAN Y., HU W. Impacts of rainfall intensity and slope gradient on rill erosion processes at loessial hillslope. Soil Tillage Research, **155**, 429, **2016**.
6. RAINATO R., MAO L., GARCIA-RAMA A., PICCO L., CESCA M., VIANELLO A., PRECISO E., SCUSSEL G.R., LENZI M.A. Three decades of monitoring in the Rio Cordon instrumented basin: Sediment budget and temporal trend of sediment yield. Geography, **291**, 45, **2017**.
7. LOPEZ-TARAZON J.A., BATALLA R.J., VERICAT D. In channel sediment storage in a highly erodible catchment: the River Isábena (Ebro Watershed, Southern Pyrenees). Geography, **55** (3), 365, **2011**.
8. NADAL-ROMERO E., MARTINEZ-MURILLO J.F., VANMAERCKE M., POESEN J. Scale-dependency of sediment yield from badland areas in Mediterranean environments. Progress in Physical Geography, **35** (3), 297, **2011**.
9. LUCIA A., LARONNE, J.B., MARTIN-DUQUE J.F. Geodynamic processes on sandy slope gullies in central Spain field observations, methods and measurements in a singular system. Geodin. Acta, **24**, 61, **2011**.
10. MARTÍN-MORENO C., FIDALGO HIJANO C., MARTÍN DUQUE J.F., GONZÁLEZ MARTÍN J.A., ZAPICO ALONSO I., LARONNE J.B. The Ribagorda sand gully (east-central Spain): Sediment yield and human-induced origin. Geomorphology, **224**, 122, **2014**.
11. LI Y., WANG Y., TANG C., OFOSU ANIM D., NI L., YU Z., ACHARYA K. Measurements of erosion rate of undisturbed sediment under different hydrodynamic conditions in lake Taihu, China. Pol. J. Environ. Stud., **23** (4), 1235, **2014**.
12. LOPEZ SAEZ J., CORONA C., STOFFEL M., ROVÉRA G., ASTRADE L., BERGER F. Mapping of erosion rates in marly badlands based on a coupling of anatomical changes in exposed roots with slope maps derived from LiDAR data. Earth Surf. Process. Landforms, **36**, 1162, **2011**.
13. VERGARI F., DELLA SETA M., DEL MONTE M., BARBIERI M. Badlands denudation "hot spots": The role of parent material properties on geomorphic processes in 20-years monitored sites of Southern Tuscany (Italy). Catena, **106**, 31, **2013**.
14. BIERBAB P., WUNDSCH M., MICHALZIK B. The impact of vegetation on the stability of dispersive material forming biancane badlands in Val de Orica, Tuscany, Central Italy. Catena, **113**, 260, **2014**.
15. CALVO-CASES A., BOIX-FAYOS C., IMESON A.C. Runoff generation, sediment movement and soil water behavior on calcareous (limestone) slopes of some Mediterranean environments in southeast Spain. Geomorphology, **50**, 269, **2003**.
16. CANTON Y., SOLE-BENET A., DE VENTE J., BIOX-FAYOS C., CALVO-CASES A., ASENSIO C., PUIGDEFÁBREGAS J. A review of runoff generation and soil erosion across scales in semiarid south-eastern Spain. Journal of Arid Environments, **75** (12), 1254, **2011**.
17. MORENO-DE LAS HERAS M., Gallart F. Lithology controls the regional distribution and morphological diversity. Geomorphology, **273**, 107, **2016**.
18. ROMERO-DIAZA A., RUIZ-SINOGAB J.D., ROBLEDANO-AYMERICHC F., BREVIKD E.C., CERDA A. Ecosystem responses to land abandonment in Western Mediterranean Mountains. Catena, **149**, 824, **2017**.
19. YETEMEN O., ISTANBULLUOGLU E., VIVONI E.R. The implications of geology, soils, and vegetation on landscape morphology: Inferences from semi-arid basins with complex vegetation patterns in Central New Mexico, USA. Geography, **116**, 246, **2010**.
20. DEFERSHA M.B., MELESSE A.M. Effect of rainfall intensity, slop and antecedent moisture content on sediment concentration and sediment enrichment ratio. Catena, **90**, 47, **2012**.
21. LIU D., SHE D., YU S., SHAO G., CHEN D. Rainfall intensity and slope gradient effects on sediment losses and splash from a saline-sodic soil under coastal reclamation. Catena, **128**, 54, **2015**.
22. NAZIR R., GHAREH S., MOSALLANEZHAD M., MOAYEDI H. The influence of rainfall intensity on soil loss mass from cellular confined slopes. Measurement, **81**, 13, **2016**.
23. DUIKER S.W., FLANAGAN D.C., LAL R. Erodibility and infiltration characteristics of five major soils of Southwest Spain. Catena, **45** (2), 103, **2001**.
24. FILEKESH E. Vegetation Type of Kashmar area in Ecological Regions of Iran. Islamic Republic of Iran, Research Institute of Forest and Rangelands, Tehran, Iran, **1995** [In Persian].
25. IAGO. Topography map of 1:50000 scale. Iranian Army Geographical Organization, Tehran, Iran, **1970**.
26. VAHABI J., NIKKAMI D. Assessing dominant factors affecting soil erosion using a portable rainfall simulator. Int. J. Sed. Res., **23**, 376, **2008**.
27. GEE G.W., OR D. Particle size analysis. In: Methods of Soil Analysis, Part 4, Eds. by J.H. Dane and G.C. Topp, SSA: Madison, USA, 255, **2002**.

28. CANTON Y., SOLE-BENET A., QUERALT I., PINI R. Weathering of a gypsum-calcareous mudstone under semi-arid environment at Tabernas, SE Spain: laboratory and field-based experimental approaches. Catena, **44**, 111, **2001**.
29. PARDINI A.G. Temporal evolution of the surface microtopography, the micromorphology and structure in relation to the weathering processes in the smectite marl of Vallcebre. PhD Thesis, University of Barcelona, Spain, 409 **1996** [In Spanish].
30. EL KATEB H., ZHANG H., ZHANG P., MOSANDL R. Soil erosion and surface runoff on different vegetation covers and slope gradients: a field experiment in Southern Shaanxi Province, China. Catena, **105**, 1, **2013**.
31. KANECAN J., KONECNA A., PODHRAZSKA J., KUCERA J. Erosion Processes and Sediment Transport during Extreme Rainfall-Runoff Events in an Experimental Catchment. Pol. J. Environ. Stud., **23**, 4, 1195, **2014**.
32. MARTINEZ-ZAVALA L., JORDAN A. Effect of rock fragment cover on interrill soil erosion from bare soils in Western Andalusia, Spain. Soil Use and Management, **24**, 108. **2008**.
33. GUMIERE S.J., BISSONNAIS Y.L, RACLOT D. Soil resistance to interrill erosion: Model parameterization and sensitivity. Catena, **77**, 274, **2009**.
34. VERMANG J., DEMEYER V., CORNELIS W. M., GABRIELS D. Aggregate stability and erosion response to antecedent water content of a loess soil. Soil Science Society of America Journal, **73**, 718, **2009**.
35. LI X.Y., CONTRERAS S., SOLE-BENET A., CANTON Y., DOMINGO F., LAZARO R., LIN H., WESEMAEL B. V., PUIGDEFABREGAS J. Controls of infiltration-runoff processes in Mediterranean karst rangelands in SE Spain. Catena, **86**, 98, **2011**.
36. ZIADAT F. M., TAIMEH A.Y. Effect of rainfall intensity, slope, land use and antecedent soil moisture on soil erosion in an arid environment. land degradation and development, **24**, 582, **2013**.
37. DE SANTIS F., GIANNOSSI M.L., MEDICI L., SUMMA V., TATEO F. Impact of physico-chemical soil properties on erosion features in the Aliano area (Southern Italy). Catena, **81**, 172, **2010**.
38. PULICE I., CAPPADONIA C., FABIO S., ROBUSTELLI G., CONOSCENTI C., DE ROSE R., ROTIGLIANO E., AGNESI V. Geomorphological, chemical and physical study of “calanchi” landforms in NW Sicily (southern Italy). Geomorphology, **153**, 219, **2012**.